Nano Energy 100 (2022) 107503

Contents lists available at ScienceDirect

Nano Energy

journal homepage: www.elsevier.com/locate/nanoen

Utilising the triboelectricity of the human body for human-computer interactions☆

Renyun Zhang [a,*], Magnus Hummelgård [a], Jonas Örtegren [a], Martin Olsen [a], Henrik Andersson [b], Ya Yang [c,d], Håkan Olin [a], Zhong Lin Wang [a,c,d,e]

[a] Department of Natural Sciences, Mid Sweden University, Holmgatan 10, SE 851 70 Sundsvall, Sweden
[b] Department of Electronics Design, Mid Sweden University, Holmgatan 10, SE 851 70, Sundsvall, Sweden
[c] CAS Center for Excellence in Nanoscience, Beijing Key Laboratory of Micro-nano Energy and Sensor, Beijing Institute of Nanoenergy and Nanosystems, Chinese Academy of Sciences, Beijing 101400, PR China
[d] Beijing Institute of Nanoenergy and Nanosystems, Chinese Academy of Sciences, Beijing 100083, PR China
[e] School of Materials Science and Engineering, Georgia Institute of Technology, Atlanta, Georgia, 30332-0245, USA

ARTICLE INFO

Keywords:
Triboelectricity
Human body
Human-computer interactions
Text inputs
Graphical input
Mouse functions

ABSTRACT

Human-computer interaction (HCI) strategies communicate the human mind and machine intelligence based on different devices and technologies. The majority of HCI strategies assume normal physical conditions that limit accessibility for users with disabilities. Certain products, such as Braille keyboards, work fine for people with specific disabilities. However, a more general HCI strategy that can neglect users' physical conditions would enhance the accessibility of these tools for disabled persons. Here, we report an HCI strategy that utilises triboelectricity of the human body (TEHB) for HCI. The TEHB can be generated by many parts of the human body, eliminating the obstacles imposed by physical function disabilities. Such an HCI approach has been used for text inputs, graphical inputs, and mimicked mouse functions. With the assistance of deep learning, an accuracy of approximately 98.4 % is achieved for text inputs obtained directly from handwriting. Our findings provide a new approach for HCI and demonstrate the feasibility of multiple interaction modes.

1. Introduction

Modern human-computer interaction (HCI) [1] techniques utilise the visual [2,3], electric [4–6] and acoustic signals [7–10] generated by users to communicate with computers. Visual-based methods capture the human body's motions or gestures [2] and interpret these signals into different pieces of information. Electric signals are usually generated on sensors such as keyboards that can be triggered by body motions. Voices, as acoustic signals, have been widely used for HCI, especially in smartphones [11]. In addition, the interactions between body motions and optical signals have also been utilised for HCI methods, such as virtual keyboards [12,13].

Most HCI strategies and products work perfectly for normal people but not for people with disabilities [14]. The needs of people with disabilities are different [15] due to the diversity of their functional losses. Strategies that are dedicated to disabled persons have been developed. For example, a Braille keyboard [16,17] was invented to help people with vision impairments communicate with computers. More recently, a brain-computer interface [11] was created by embedding microelectrodes into the brain for brain-to-text communication via handwriting, achieving an accuracy greater than 99 %. Although efforts have been made to improve HCI mechanisms for disabled persons, a challenge remains: developing a strategy that uses simple signal acquisition methods and requires body motions that are as simple as possible. Such a strategy can increase the accessibility and universal access of HCI methods [18].

Here, we report a strategy to utilise the human body's triboelectricity (TEHB) [19–21] for performing HCI (TEHB-HCI). TEHB signals can be generated by many movable parts of the body, such as the fingers, elbows, and feet, and these signals can be sensed by using either a wired

☆ "Prof Zhong Lin Wang, an author on this paper, is the Editor-in-Chief of Nano Energy, but he had no involvement in the peer review process used to assess this work submitted to Nano Energy. This paper was assessed, and the corresponding peer review managed by Professor Chenguo Hu, also an Associate Editor in Nano Energy"

* Corresponding author.
E-mail address: renyun.zhang@miun.se (R. Zhang).

https://doi.org/10.1016/j.nanoen.2022.107503
Received 17 May 2022; Received in revised form 7 June 2022; Accepted 11 June 2022
Available online 15 June 2022

method or a wireless method. HCI activities such as text inputting, graphical inputting and mouse functions have been successfully performed. High-accuracy text inputting was realised by using a trained convolutional neural network (CNN) model and a linear discriminant analysis (LDA) model. Feasible graphical inputting has been demonstrated by using a wireless sensing strategy that directly interprets finger drawings of simple graphics on a tribolayer into shapes on a computer screen. Moreover, mimicked mouse functions have been realised based on a noncontact wireless sensing strategy.

2. Results

2.1. Wired and wireless sensing of the TEHB

The triboelectrification between the skin and the tribolayer caused charge separation at the interface, leading to charge accumulation on the human body and the tribolayer that built up potentials [20]. To measure this potential, we developed wired and wireless methods that were recently used in different HCI scenarios.

For the wired method (Fig. 1a, Fig. S1a), an electrostatic discharge (ESD) wrist strap was placed on the wrist of a participant to generate charges on the human body. The other terminal of the strap was connected to a digital multimeter and then to the ground. In this way, the potential difference between the human body and the ground was measured, which could be used to record the TEHB while performing handwriting with continuously changing forces and contact areas between the finger and the tribolayer (Fig. 1b). In this way, the writing of a specific text produced a unique signal pattern that could later be identified based on machine learning models.

For the wireless measurement approach (Fig. 1c, Fig. S1b), an Arduino Nano programmed as a voltmeter was placed close to a tribolayer to sense the potential changes between the human body and the tribolayer. For the case in which no background change was observed, the interaction mode could be simplified as shown in Fig. 1d. The change in the distance (d) between the skin and the tribolayer changed the potential of the human body (V_H) because the charge generated on the skin had the possibility to move on the human body. A change in d did not change the potential of the tribolayer (V_T) if no physical contact had been made because the charges stayed at the surface of the tribolayer without moving. However, if physical contact occurred between the skin and the tribolayer, both V_H and V_T changed. In both scenarios, the electric fields produced by the two surfaces changed, resulting in signal changes on the sensor. Simply, the potential can be estimated by an equation:

$$V_S = C(V_H - V_T)/d_{HT-S}$$

where V_S is the sensed potential on the sensor, $d_{HT\text{-}S}$ is the distance between the sensor and the edge of the V_H/V_T system, and C is a constant.

2.2. Text input from handwriting

Handwriting, specifically finger writing in this study, is a highly repeatable body movement (Fig. S2); therefore, it is possible to recognise handwriting by analysing the features of the associated TEHB signals. Two approaches were developed to realise text inputs by using CNNs [22] and the combination of dynamic time warping (DTW) [23,

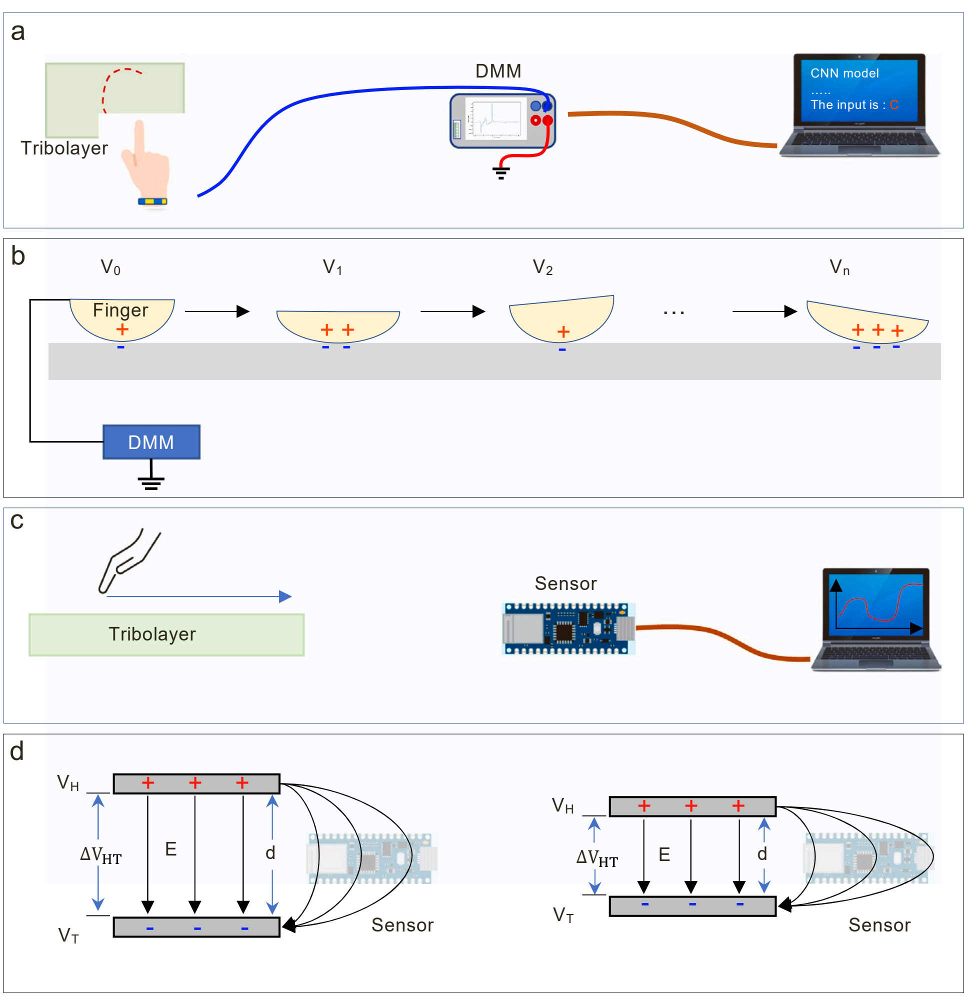

Fig. 1. Sensing mechanism of the TEHB. (a) A schematic drawing of the wired TEHB sensing process, where an ESD strap was worn and connected to the ground through a digiatal multimeter (DMM). The potential between the body and the ground was measured while a finger was writing on a tribolayer. (b) The charge generation process of handwriting on a tribolayer. The changes in the pressure and contact area led to changes in the potential on the body. (c) A schematic drawing of the wireless TEHB sensing process, where a sensor connected to a computer was placed near a tribolayer. (d) A schematic drawing of the mechanism of the wireless sensing method. The changes in the electric field built between the body and the tribolayer resulted in different sensor signals.

24] and linear discriminant analysis (LDA).

The CNN model (Fig. 1a) included three Conv1D layers with filters and kernel sizes of (64, 100), (128, 100) and (256, 100). A pooling layer (GlobalAveragePooling1D) and a dense layer were added after the Conv1D layers. The built model was trained and tested with handwriting data including both uppercase and lowercase English letters. To visualise the multidimensional time series data on a 2D plot, *t*-distributed stochastic neighbour embedding (*t*-SNE) [25] was applied after each layer of the CNN model. Fig. 2b and c show the *t*-SNE plots of the uppercase and lowercase letters of the output derived from the CNN model, indicating 26 clusters that represent the 26 letters.

The accuracies of the CNN model on the training datasets reached 99.7 %, while the loss was lower than 0.1. The accuracies on the test sets were 97.1 % for uppercase letters (Figs. 2d) and 98.4 % for lowercase letters (Fig. 2e). Plots of the accuracies and losses versus the number of epochs are given in Fig. S3. The results demonstrated the high accuracy of determining text inputs from handwriting via the CNN model.

Instead of extracting the features from the signals, we used DTW to calculate the similarities of the TEHB signals (Fig. 3a~d) of uppercase and lowercase letters (Fig. S4), and the DTW distances (Fig. 3e, f) were used as features to train an LDA model. We also applied *t*-SNE to visualise the clusters of the DTW distances for both uppercase and lowercase letters (Fig. 3g, h). The test accuracies were 97.4 % for uppercase letters and 97.7 % for lowercase letters. The receiver operating characteristic (ROC) curves shown in Fig. 3i and j and the areas under the curve [26] (AUCs) equal to 1 indicated the high performance of the proposed method. Comparing to the CNN based model, the DTW-LDA model has a shorter training time while remaining a compatible high accuracy.

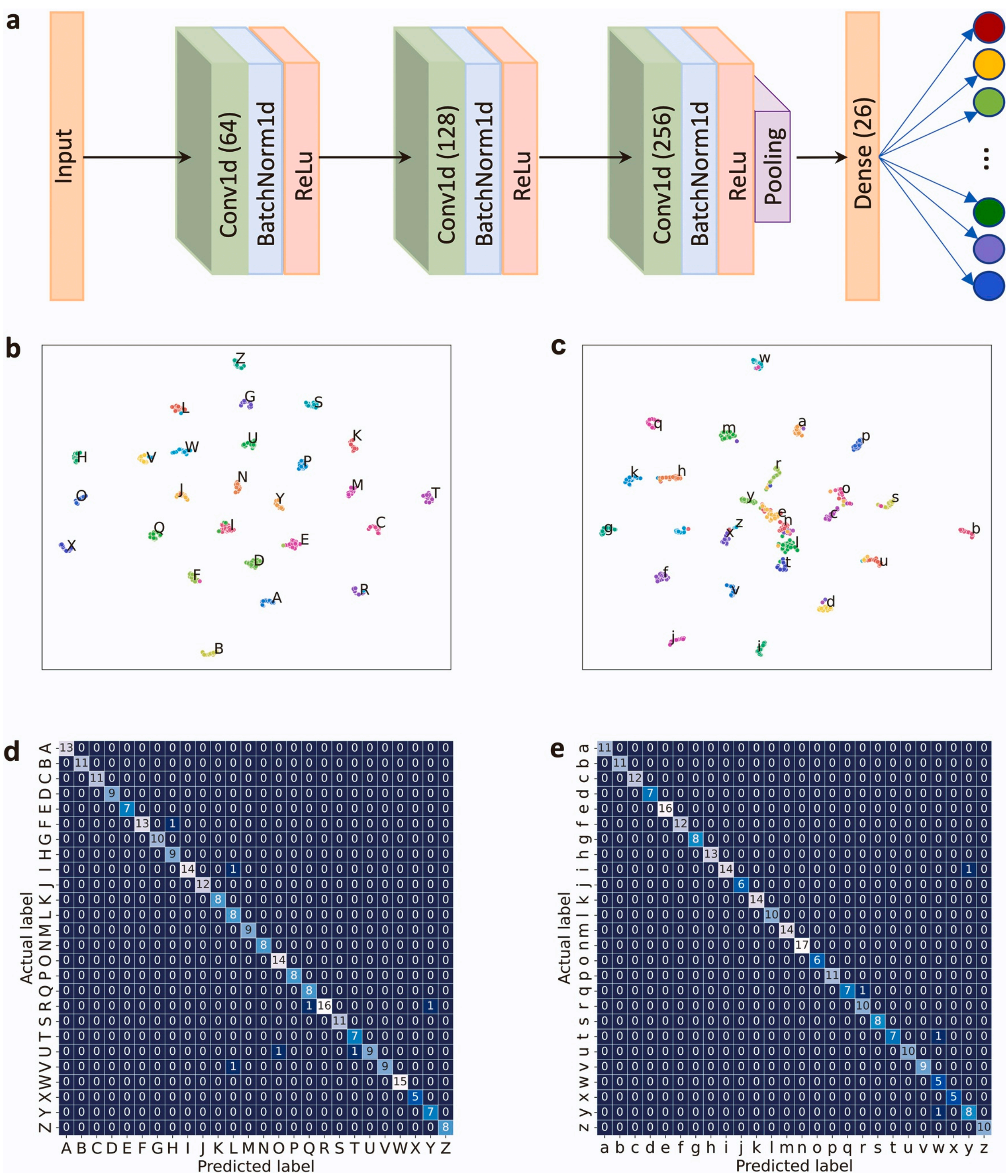

Fig. 2. The Conv1D model for text input. (a) The structure of the Conv1D model containing three layers. (b) and (c) *t*-SNE visualisations of the output of the Conv1D model for handwritten uppercase and lowercase letters. The dimensionality of the data was reduced to 10 via PCA before applying *t*-SNE. (d) and (f) The confusion matrices obtained on the test subset by using the trained Conv1D model, achieving accuracies of 97.1 % and 98.4 % for uppercase and lowercase letters, respectively.

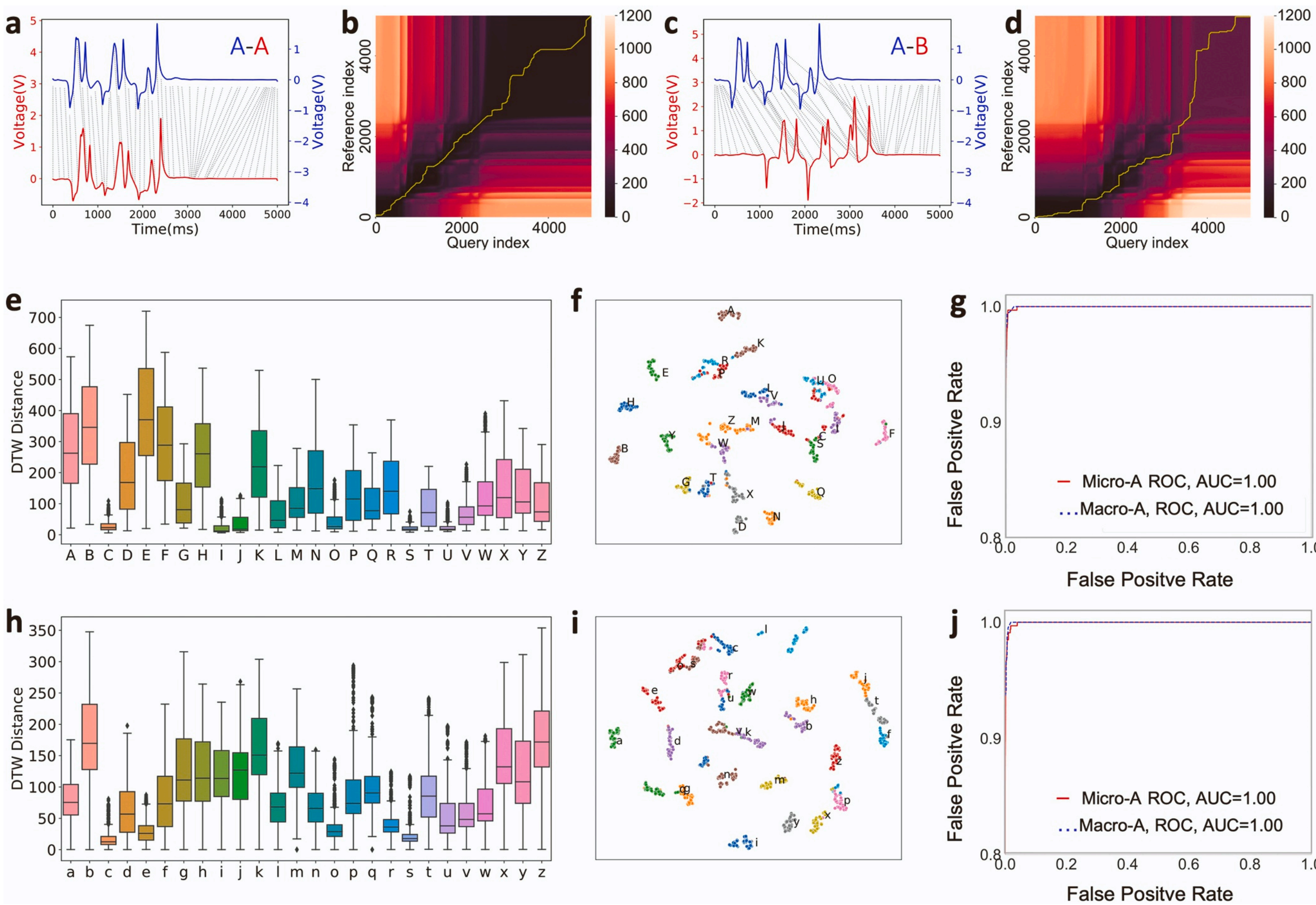

Fig. 3. DTW-LDA model for text input. (a) DTW distance between two TEHB signals of handwritten samples of the uppercase letter "A", showing the line matches. (b) The warp path of the DTW result in (a). (c) DTW distance between the TEHB signals of handwritten uppercase letters "A" and "B", showing the line matches. (d) The warp path of the DTW result in (c). (e) Box plot of the DTW distances among the measured signals for the handwritten uppercase letters and the signals in the database. (f) *t*-SNE visualisation of the DTW distances in (e). (g) ROC plot of the LDA model, showing the micro-averages (Micro-A) and macro-averages (Macro-A) and the AUC values. (h) Box plot of the DTW distances among the measured signals for the handwritten lowercase letters and the signals in the database. (i) *t*-SNE visualisation of the DTW distances in (h). (j) ROC plot of the LDA model, showing the Micro-A, Macro-A and the AUC values.

2.3. Code-based wireless text inputs

In addition to the direct interpretation of handwriting, the indirect translation of codes was also investigated for text inputs. Here, the peaks of the TEHB signals were sensed wirelessly and utilised for assigning "1" or "0" based on their intensities compared to a threshold. Higher intensities ("1") above the threshold were generated by tapping with two fingers, while lower-intensity ("0") signals were generated by tapping with one finger. Another alternative is to use materials with higher triboelectric effects, such as PTFE and PFA, to generate high-intensity signals and use materials with lower triboelectric effects, such as PET and PEI, to generate low-intensity signals. Different code systems (Fig. 4a), such as Morse, Braille, and binary codes, were tested, and the accuracy was approximately 99 % (99 of 100 tests). In addition, a self-designed code system (Fig. 4b and c) could also be applied for text inputs, giving the users more personality and security in their text inputs. This type of code-based input could be performed on different surfaces that are easily accessible (Fig. 4d) and even on wet surfaces (Fig. 4e), indicating the feasibility of the strategy.

2.4. Wireless graphical inputs

Graphical inputting is another important HCI activity that has been performed with different methods based on touch screen sensors [27] or parameter settings in software. Position sensors can trace the movement of a hand and produce a graphical structure. Command-based methods give orders to the computer to draw graphical structures. The TEHB-HCI-based graphical input strategy combines the advantages of the above two methods. Such a method can sense the movement of the hand but does not trace its positions, and it extract features from signals as commands to draw graphical structures. Generally, communications are based on the number of peaks, the widths of the peaks, and the distances among the peaks. For example, a finger drawing of a circle produces two peaks that are different from the three peaks produced by a triangle (Fig. 5a and b). Based on the widths of the peaks, we made simple algorithms to set the parameters of different shapes (Fig. 5c). Supporting Information V1 shows a video about how the graphical inputs were collected. The reason why the widths of the peaks were used to set the parameters of the shapes is because they directly reflected the movements of the finger, where a longer movement led to a wider peak that resulted in, e.g., a longer rectangle side than that yielded by a shorter finger movement. That said, the parameters of the graphics could be easily tuned by the widths of the peaks, which are practically determined by the speeds and the periods of finger movements. By adding more settings to the program, we created more complex graphical patterns (Fig. 5d).

Supplementary material related to this article can be found online at doi:10.1016/j.nanoen.2022.107503.

In addition to the use of the peak widths to set the parameters of the different shapes, one can also use the distances between the peaks to set

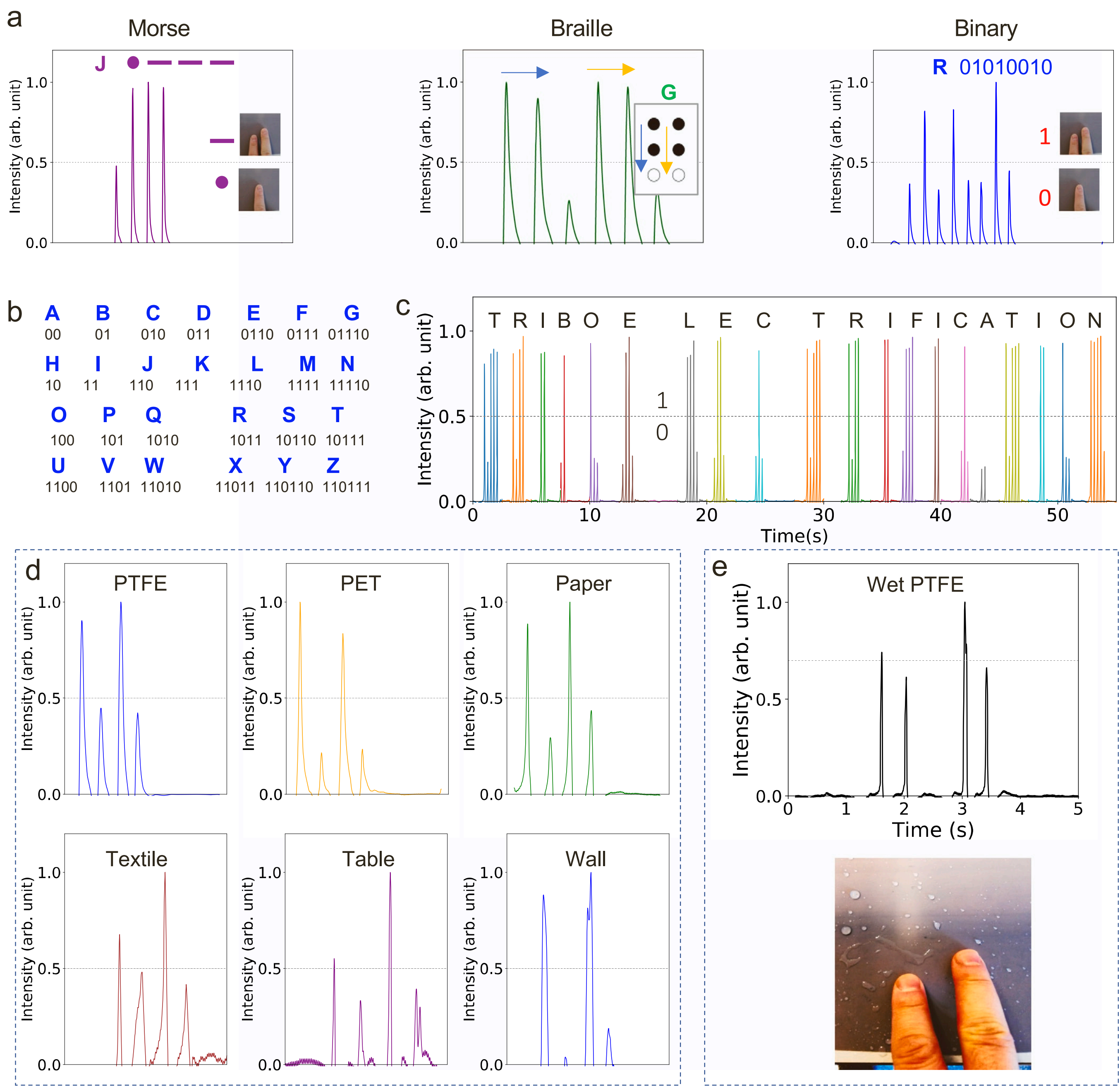

Fig. 4. Code-based text inputs. (a) TEHB-based text input obtained by using Morse, Braille and binary code systems. The stronger signals with intensities above 0.5 generated by tapping with two fingers are represented as dashes, black dots and "1"s in the Morse, Braille and binary code systems, respectively. The weaker signals with intensities below 0.5 generated by tapping with one finger are represented dots, the white dots and "0"s in the Morse, Braille and Binary code systems, respectively. (b) A homemade code system. (c) The input of the word "TRIBOELECTRIFICATION" based on the homemade code system. (d) TEHB-based text inputs produced on different surfaces. The code represents the letter "Q" in the homemade code system. (e) Text inputting on a wet PTFE surface, showing the corresponding TEHB signal and a photograph of the surface.

these parameters (Fig. S5. The peaks could be generated by finger tapping instead of drawing. Although this approach does not directly interpret finger drawings, it has more controllable parameter settings. The reason for this is that the distances between the peaks are more certain than the peak widths, which are highly dependent on the preassigned settings in the program and can be influenced by the neighbour peaks.

2.5. *Mimicked mouse functions*

TEHB signals have also been used to realize mouse functions based on the features of the TEHB signals. To improve the user experience, a nontouch-based wireless method (Fig. 1d) was developed so that the hand could move freely. Such a strategy afforded a new user representation method [29]. Mouse functions, such as cursor control and left and right clicks, were successfully performed based on the obtained TEHB signals, as shown in Fig. 6. The TEHB signals with single peaks (Fig. 6a, b) were used to move the cursor vertically, and the widths of the peaks

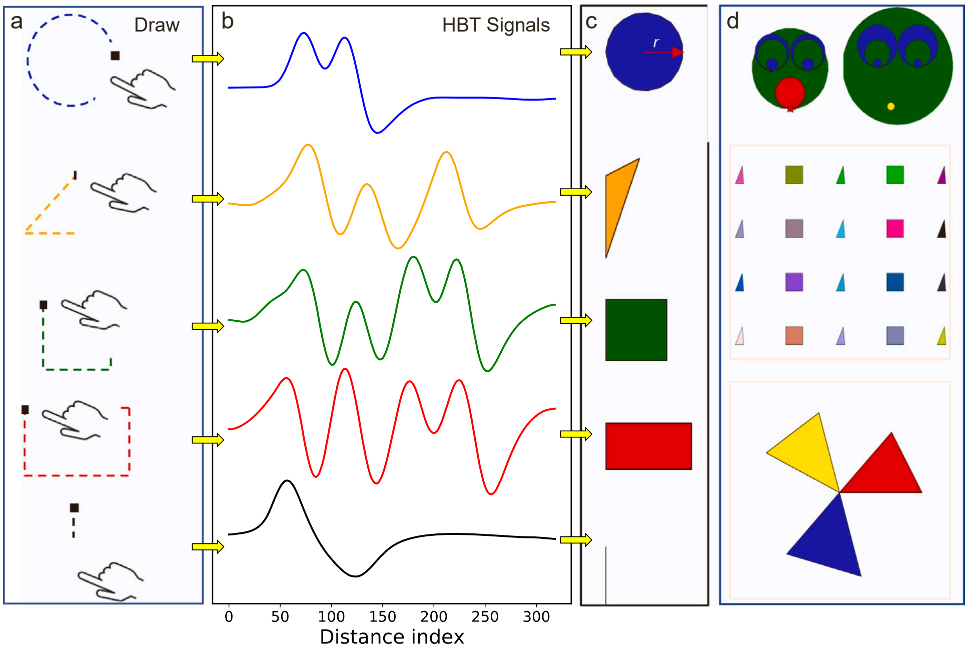

Fig. 5. Graphical inputs based on a wireless TEHB-HCI strategy. (a) The movement of a finger on a tribolayer for generating TEHB signals to be interpreted into shapes on a screen. (b) The specific TEHB signals for the shapes in (a). The full widths of the peaks extracted by using the SciPy [28] signal processing toolbox and used as distance indices for the created shapes. (c) Shapes created on a screen based on the features of the TEHB signals. The lengths of the sides and the line were calculated based on the widths of the peaks. (d) Different figures and patterns created by using the TEHB-based graphical inputs.

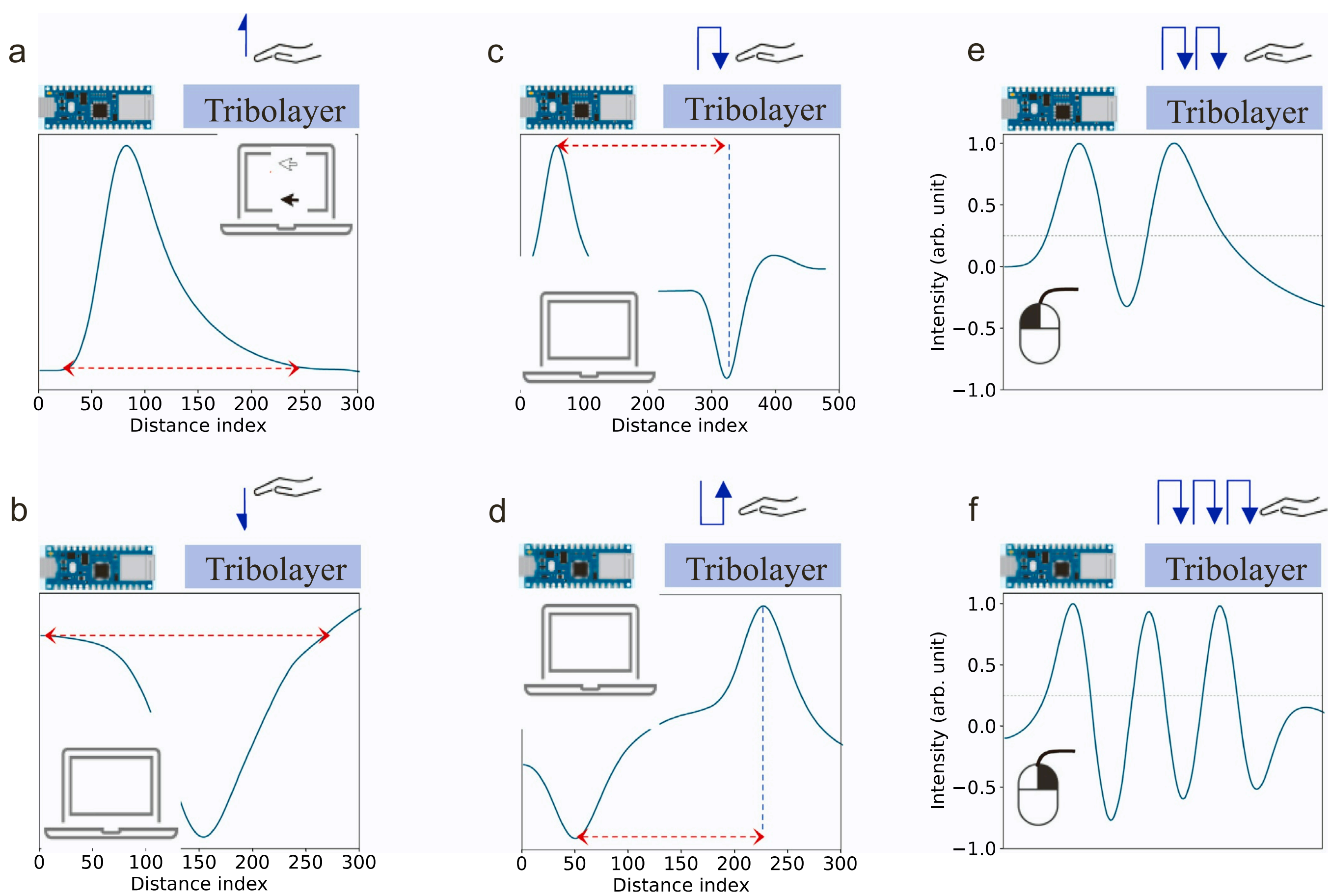

Fig. 6. Mouse functions based on a wireless TEHB-HCI strategy without touching. (a) Moving a hand away from a tribolayer, generating a positive peak that was interpreted as an upwards cursor movement. The width of the peak was used as a distance index for cursor movement. (b) Moving a hand close to a tribolayer, generating a negative peak that was interpreted as a downwards cursor movement. (c) Moving a hand first up and then down, generating a signal for moving the cursor to the right. The distance between the peaks was used as the cursor movement distance. (d) Moving a hand first down and then up, generating a signal for moving the cursor to the left. (e) and (f) Moving a hand up and down quickly two or three times. The number of peaks was used as a feature, where 2 peaks (e) equalled a left click and 3 peaks (f) equalled a right click.

were used as the distance index for cursor movement. In this study, we directly turned the peak widths in milliseconds into pixels for positioning the cursor. The TEHB signals with positive and negative peaks (Fig. 5c, d) were used to move the cursor horizontally based on the peak that came first, and the distances between the peaks were used as the distance index. With these four basic movements, one could manipulate the cursor on a screen. The left and right clicks of a mouse were also realised in a simple manner by counting the numbers of positive peaks. The TEHB signals with two peaks were interpreted as left clicks, and the signals with three peaks were interpreted as right clicks. Supporting Information V2 shows a video of the experiments.

2.6. Perform TEHB-HCI by different body parts

The physical mechanism behind the TEHB decides that it can be performed by any part of the human body. In most of the scenarios, it is the part on upper and lower limbs that are used. In our experiments (Fig. S6), triboelectric signals that generated by finger, thenar and hypothenar eminences, elbow, toe, and heel have been successfully collected with good enough signal to noise ratio. Such results implies that the TEHB-HCI strategy is not limited by the physical functions of the users, making it a universe way of the HCI.

3. Discussion

It should be noted that TEHB signals have strong personal characteristics, making the TEHB-HCI approach produce strong personalities that play a prominent role in HCI [30]. A simple example is how users write the letter "A". Some users write in two strokes, while others write in three strokes (Fig. S7). The TEHB-HCI method allows users to have personalised writing habits that might not be achievable with other types of HCI. To make a more general model that can be applied for multiple users, there is a need to collect handwriting data from different persons.

The personalised [31] TEHB-HCI approach leads to higher levels of security [18] and privacy [32] than those achieved by other methods, such as keyboard-based HCI. For example, a user can build a specific code system by using different TEHB signal features, which have a high level of security.

During the experiments, we found that the TEHB signals could present the user's moods (Fig. S8), which may lead to a new affective computing strategy [33,34] in which emotion recognition [35,36] is the essential component. Different from the currently used vision- or voice-based emotion recognition methods [9,35], the TEHB-HCI technique requires no extra device, such as a camera [3,37,38], and uses less space. This will lead to new studies in artificial intelligence.

Currently used HCI strategies are generally for people with normal physical functions which may due to the limited market of products. Another reason is the diverse of disabilities. For example, the keyboard for text input with Braille code could not serve people with hand or finger related disabilities. There are many other types of triboelectric sensors based HCI, such as TENG based tactile sensors [39–41] and TENG based keyboards [42,43], and other types devices such as electronic skins [44,45], etc. comparing to these sensors, the advantages of the TEHB-HCI are the simplicity of the device, high accessibility, the availability of materials, and the low demand of physical functions. The disadvantages are the highly dependent on machine learning algorithm and the sensitivity background noises.

4. Conclusion

In summary, we presented a new HCI method based on the TEHB. The human minds represented by triboelectric signals could be directly read and translated by computer programs through different approaches, realising text inputting, graphical inputting and mouse functions. Such a strategy gives the TEHB-HCI approach more personality, as well as high levels of security and privacy. Moreover, the diversity of the material choices make the TEHB-HCI method flexible and feasible in both time and place. An TEHB-HCI method that includes emotions could lead to a new affective computing strategy. Future works may focus on improving the machine learning process to improve the efficiency and accuracy of signal interpretation.

5. Experimental section

The wired TEHB signal measurement process was performed by connecting the human body to the ground through a digital multimeter (PXI 4071). An ESD band was worn on the wrist, and the other band terminal was connected to the digital multimeter. The digital multimeter was then attached to the ground. The program for measuring the TEHB signal was homemade with a sampling ratio of 1000/s. The substrate used for handwriting was a 0.13 mm thick PTFE (High-Tech-Flon®) film glued on a desk.

For the wireless TEHB signal measurement process, an Arduino Nano that was programmed as a voltmeter was connected to a computer via a docking station. The substrate used was a piece of a PMMA board (Materialbutiken, A4 size, 3 mm thick). During the measurement procedure, the Arduino Nano was placed beside the PMMA board.

Other materials such as PEI and PET are purchased from McMaster with thicknesses of 0.05 mm.

For the nontouch-based wireless measurement process utilized to obtain the TEHB signals that were used for mimicking mouse functions, the PMMA board was precharged by hand rubbing.

The participant wore regular clothes and shoes during all the experiments. No specific attention was given to the clothing. The participant did not apply any skincare product to their skin.

Full methodology, e.g. data preparation and process is given in the supporting information: experiment.

CRediT authorship contribution statement

Renyun Zhang: Conceptualization, Methodology, Software, Writing – review – editing. **Magnus Hummelgård:** Methodology. **Jonas Örtegren:** Project administration, Funding acquisition. **Martin Olsen:** Methodology. **Henrik Andersson:** Methodology. **Ya Yang:** Writing – review & editing. **Håkan Olin:** Project administration, Funding acquisition. **Zhong Lin Wang:** Writing – review & editing.

Declaration of Competing Interest

Renyun Zhang has filed a patent application for the TEHB-HCI in the USPTO Provisional Application (US Provisional Patent Application no. 63/327,397).

Data and code Availbility

All measured HBT signals to reproduce the findings in this study are publicly available at GitHub. https://github.com/renzha-miun/HBT-HCI/tree/main/Data. Code that implements the HBT-HCI in this study is publicly available on GitHub at https://github.com/renzha-miun/HBT-HCI.

Acknowledgements

The project was financially supported by Stiftelsen Promobilia and the Knowledge Foundation of Sweden. The authors especially thank the contributors to forums such as GitHub, Kaggle, StackExchange and Arduino for their help and inspiration that have enabled the success of this work.

Appendix A. Supporting information

Supplementary data associated with this article can be found in the online version at doi:10.1016/j.nanoen.2022.107503.

References

[1] S.K. Card, T.P. Moran, A. Newell, The Psychology of Human–Computer Interaction, Lawrence Erlbaum Associates, Inc., New Jersey, 1983.
[2] C. von Hardenberg, F. Bérard, Bare-Hand Human-computer Interaction, in: Proc. 2001 work. Percetive User Interfaces - PUI '01, ACM Press, New York, New York, USA, 2001, p. 1, https://doi.org/10.1145/971478.971513.
[3] S.S. Rautaray, A. Agrawal, Vision based hand gesture recognition for human computer interaction: a survey, Artif. Intell. Rev. 43 (2015) 1–54, https://doi.org/10.1007/s10462-012-9356-9.
[4] S. Zhai, P.O. Kristensson, The word-gesture keyboard, Commun. Acm. 55 (2012) 91–101, https://doi.org/10.1145/2330667.2330689.
[5] B.W. Roysden Jr,1996. Keyboard, 5,575,576, 1996. 〈https://patents.google.com/patent/US5575576A/en〉.
[6] T. Költringer, T. Grechenig, 2004. Comparing the immediate usability of graffiti 2 and virtual keyboard, in: Ext. Abstr. 2004 Conf. Hum. Factors Comput. Syst. - CHI '04, ACM Press, New York, New York, USA, 2004: p. 1175. https://doi.org/10.1145/985921.986017.
[7] S. Ortmanns, H. Ney, X. Aubert, A word graph algorithm for large vocabulary continuous speech recognition, Comput. Speech Lang. 11 (1997) 43–72, https://doi.org/10.1006/csla.1996.0022.
[8] P. Ghahremani, B. BabaAli, D. Povey, K. Riedhammer, J. Trmal, S. Khudanpur, 2014. A pitch extraction algorithm tuned for automatic speech recognition, in: 2014 IEEE Int. Conf. Acoust. Speech Signal Process., IEEE, 2014: pp. 2494–2498. https://doi.org/10.1109/ICASSP.2014.6854049.
[9] S.K. Gaikwad, B.W. Gawali, P. Yannawar, A review on speech recognition technique, Int. J. Comput. Appl. 10 (2010) 16–24, https://doi.org/10.5120/1462-1976.
[10] P.R. Cohen, S.L. Oviatt, The role of voice input for human-machine communication, Proc. Natl. Acad. Sci. 92 (1995) 9921–9927, https://doi.org/10.1073/pnas.92.22.9921.
[11] F.R. Willett, D.T. Avansino, L.R. Hochberg, J.M. Henderson, K.V. Shenoy, High-performance brain-to-text communication via handwriting, Nature 593 (2021) 249–254, https://doi.org/10.1038/s41586-021-03506-2.
[12] H. Du, T. Oggier, F. Lustenberger, E. Charbon, 2005. A Virtual Keyboard Based on True-3D Optical Ranging, in: Procedings Br. Mach. Vis. Conf. 2005, British Machine Vision Association, 2005: pp. 27.1–27.10. https://doi.org/10.5244/C.19.27.
[13] J. Edelmann, P. Mock, A. Schilling, P. Gerjets, W. Rosenstiel, W. Straßer, 2012. Towards the keyboard of oz, in: Proc. 2012 ACM Int. Conf. Interact. Tabletops Surfaces - ITS '12, ACM Press, New York, New York, USA, 2012: p. 163. https://doi.org/10.1145/2396636.2396662.
[14] E. Mencarini, A. Rapp, L. Tirabeni, M. Zancanaro, Designing wearable systems for sports: a review of trends and opportunities in human-computer interaction, IEEE Trans. Hum. -Mach. Syst. 49 (2019) 314–325, https://doi.org/10.1109/THMS.2019.2919702.
[15] P. Biswas, D. Samanta, Friend: a communication aid for persons with disabilities, IEEE Trans. Neural Syst. Rehabil. Eng. 16 (2008) 205–209, https://doi.org/10.1109/TNSRE.2008.917305.
[16] A. Church, J. Lloyd, R. Hadsell, N.F. Lepora, Deep reinforcement learning for tactile robotics: learning to type on a braille keyboard, IEEE Robot. Autom. Lett. 5 (2020) 6145–6152, https://doi.org/10.1109/LRA.2020.3010461.
[17] M. Alnfiai, S. Sampali, 2017. An Evaluation of the BrailleEnter Keyboard: An Input Method Based on Braille Patterns for Touchscreen Devices, in: 2017 Int. Conf. Comput. Appl., IEEE, 2017: pp. 107–119. https://doi.org/10.1109/COMAPP.2017.8079740.
[18] C. Stephanidis, G. Salvendy, M. Antona, J.Y.C. Chen, J. Dong, V.G. Duffy, X. Fang, C. Fidopiastis, G. Fragomeni, L.P. Fu, Y. Guo, D. Harris, A. Ioannou, K. (Kate) Jeong, S. Konomi, H. Krömker, M. Kurosu, J.R. Lewis, A. Marcus, G. Meiselwitz, A. Moallem, H. Mori, F. Fui-Hoon Nah, S. Ntoa, P.-L.P. Rau, D. Schmorrow, K. Siau, N. Streitz, W. Wang, S. Yamamoto, P. Zaphiris, J. Zhou, Seven HCI grand challenges, Int. J. Hum. Interact. 35 (2019) 1229–1269, https://doi.org/10.1080/10447318.2019.1619259.
[19] R. Zhang, J. Örtegren, M. Hummelgård, M. Olsen, H. Andersson, H. Olin, Harvesting triboelectricity from the human body using non-electrode triboelectric nanogenerators, Nano Energy 45 (2018) 298–303, https://doi.org/10.1016/j.nanoen.2017.12.053.
[20] R. Zhang, M. Hummelgård, J. Örtegren, Y. Yang, H. Andersson, E. Balliu, N. Blomquist, M. Engholm, M. Olsen, Z.L. Wang, H. Olin, Sensing body motions based on charges generated on the body, Nano Energy 63 (2019), 103842, https://doi.org/10.1016/j.nanoen.2019.06.038.
[21] R. Zhang, M. Hummelgård, J. Örtegren, M. Olsen, H. Andersson, Y. Yang, H. Olin, Human body constituted triboelectric nanogenerators as energy harvesters, code transmitters, and motion sensors, ACS Appl. Energy Mater. 1 (2018) 2955–2960, https://doi.org/10.1021/acsaem.8b00667.
[22] Y. LeCun, Y. Bengio, G. Hinton, Deep learning, Nature 521 (2015) 436–444, https://doi.org/10.1038/nature14539.
[23] T. Giorgino, Computing and visualizing dynamic time warping alignments in r: the dtw package, J. Stat. Softw. 31 (2009) 1–24, https://doi.org/10.18637/jss.v031.i07.
[24] P. Tormene, T. Giorgino, S. Quaglini, M. Stefanelli, Matching incomplete time series with dynamic time warping: an algorithm and an application to post-stroke rehabilitation, Artif. Intell. Med. 45 (2009) 11–34, https://doi.org/10.1016/j.artmed.2008.11.007.
[25] L. van der Maaten, G. Hinton, Visualizing data using t-SNE Laurens, J. Mach. Learn. Res. 9 (2008) 2579–2650.
[26] A.P. Bradley, The use of the area under the ROC curve in the evaluation of machine learning algorithms, Pattern Recognit. 30 (1997) 1145–1159, https://doi.org/10.1016/S0031-3203(96)00142-2.
[27] M. Sun, X. Cao, H. Song, S. Izadi, H. Benko, F. Guimbretiere, X. Ren, K. Hinckley, 2011. Enhancing naturalness of pen-and-tablet drawing through context sensing, in: Proc. ACM Int. Conf. Interact. Tabletops Surfaces - ITS '11, ACM Press, New York, New York, USA, 2011: p. 83. https://doi.org/10.1145/2076354.2076371.
[28] P. Virtanen, R. Gommers, T.E. Oliphant, M. Haberland, T. Reddy, D. Cournapeau, E. Burovski, P. Peterson, W. Weckesser, J. Bright, S.J. van der Walt, M. Brett, J. Wilson, K.J. Millman, N. Mayorov, A.R.J. Nelson, E. Jones, R. Kern, E. Larson, C. J. Carey, I. Polat, Y. Feng, E.W. Moore, J. VanderPlas, D. Laxalde, J. Perktold, R. Cimrman, I. Henriksen, E.A. Quintero, C.R. Harris, A.M. Archibald, A.H. Ribeiro, F. Pedregosa, P. van Mulbregt, A. Vijaykumar, A. Pietro Bardelli, A. Rothberg, A. Hilboll, A. Kloeckner, A. Scopatz, A. Lee, A. Rokem, C.N. Woods, C. Fulton, C. Masson, C. Häggström, C. Fitzgerald, D.A. Nicholson, D.R. Hagen, D. V. Pasechnik, E. Olivetti, E. Martin, E. Wieser, F. Silva, F. Lenders, F. Wilhelm, G. Young, G.A. Price, G.-L. Ingold, G.E. Allen, G.R. Lee, H. Audren, I. Probst, J. P. Dietrich, J. Silterra, J.T. Webber, J. Slavič, J. Nothman, J. Buchner, J. Kulick, J. L. Schönberger, J.V. de Miranda Cardoso, J. Reimer, J. Harrington, J.L. C. Rodríguez, J. Nunez-Iglesias, J. Kuczynski, K. Tritz, M. Thoma, M. Newville, M. Kümmerer, M. Bolingbroke, M. Tartre, M. Pak, N.J. Smith, N. Nowaczyk, N. Shebanov, O. Pavlyk, P.A. Brodtkorb, P. Lee, R.T. McGibbon, R. Feldbauer, S. Lewis, S. Tygier, S. Sievert, S. Vigna, S. Peterson, S. More, T. Pudlik, T. Oshima, T.J. Pingel, T.P. Robitaille, T. Spura, T.R. Jones, T. Cera, T. Leslie, T. Zito, T. Krauss, U. Upadhyay, Y.O. Halchenko, Y. Vázquez-Baeza, SciPy 1.0: fundamental algorithms for scientific computing in python, Nat. Methods 17 (2020) 261–272, https://doi.org/10.1038/s41592-019-0686-2.
[29] S. Seinfeld, T. Feuchtner, A. Maselli, J. Müller, User representations in human-computer interaction, Hum. Interact. 36 (2021) 400–438, https://doi.org/10.1080/07370024.2020.1724790.
[30] C. Nass, Y. Moon, B.J. Fogg, B. Reeves, C. Dryer, Can computer personalities be human personalities?, in: Conf. Companion Hum. Factors Comput. Syst. - CHI '95, ACM Press, New York, New York, USA, 1995: pp. 228–229. https://doi.org/10.1145/223355.223538.
[31] M. Augstein, E. Herder, W. Wörndl, Personalized human-computer interaction, De. Gruyter Oldenbourg (2019), https://doi.org/10.1515/9783110552485.
[32] G. Iachello, J. Hong, End-user privacy in human-computer interaction, Found. Trends® Hum. -Comput. Interact. 1 (2007) 1–137, https://doi.org/10.1561/1100000004.
[33] R.W. Picard, Affective Computing, The MIT Press, Cambridge, Massachusetts, 2000.
[34] S. Balters, M. Steinert, Capturing emotion reactivity through physiology measurement as a foundation for affective engineering in engineering design science and engineering practices, J. Intell. Manuf. 28 (2017) 1585–1607, https://doi.org/10.1007/s10845-015-1145-2.
[35] M. Ali, A.H. Mosa, F. Al Machot, K. Kyamakya, Emotion Recognition Involving Physiological and Speech Signals: A Comprehensive Review, in: Recent Advances Nonlinear Dynamics and Synchronization, Springer, Cham, 2018, pp. 287–302, https://doi.org/10.1007/978-3-319-58996-1_13.
[36] Y. Li, Y. Jiang, D. Tian, L. Hu, H. Lu, Z. Yuan, AI-enabled emotion communication, IEEE Netw. 33 (2019) 15–21, https://doi.org/10.1109/MNET.001.1900070.
[37] C. Von Hardenberg, F. Bérard, 2018. Bare-Hand Human-Computer Interaction, n.d. 〈http://citeseerx.ist.psu.edu/viewdoc/download?doi=10.1.1.23.4541&rep=rep1&type=pdf〉 (Accessed October 26, 2018).
[38] A. Erol, G. Bebis, M. Nicolescu, R.D. Boyle, X. Twombly, A Review on Vision-Based Full DOF Hand Motion Estimation, in: 2005 IEEE Comput. Soc. Conf. Comput. Vis. Pattern Recognit. - Work., IEEE, n.d.: pp. 75–75. https://doi.org/10.1109/CVPR.2005.395.
[39] X. Pu, Q. Tang, W. Chen, Z. Huang, G. Liu, Q. Zeng, J. Chen, H. Guo, L. Xin, C. Hu, Flexible triboelectric 3D touch pad with unit subdivision structure for effective XY positioning and pressure sensing, Nano Energy 76 (2020), 105047, https://doi.org/10.1016/j.nanoen.2020.105047.
[40] X. Pu, M. Liu, X. Chen, J. Sun, C. Du, Y. Zhang, J. Zhai, W. Hu, Z.L. Wang, Ultrastretchable, transparent triboelectric nanogenerator as electronic skin for biomechanical energy harvesting and tactile sensing, Sci. Adv. 3 (2017) 1689, https://doi.org/10.1126/sciadv.1700015.
[41] D.H. Ho, J. Han, J. Huang, Y.Y. Choi, S. Cheon, J. Sun, Y. Lei, G.S. Park, Z.L. Wang, Q. Sun, J.H. Cho, β-Phase-Preferential blow-spun fabrics for wearable triboelectric nanogenerators and textile interactive interface, Nano Energy 77 (2020), 105262, https://doi.org/10.1016/j.nanoen.2020.105262.
[42] J. Yi, K. Dong, S. Shen, Y. Jiang, X. Peng, C. Ye, Z.L. Wang, Fully fabric-based triboelectric nanogenerators as self-powered human–machine interactive keyboards, Nano-Micro Lett. 13 (2021) 1–13, https://doi.org/10.1007/s40820-021-00621-7.

[43] S.B. Jeon, S.J. Park, W.G. Kim, I.W. Tcho, I.K. Jin, J.K. Han, D. Kim, Y.K. Choi, Self-powered wearable keyboard with fabric based triboelectric nanogenerator, Nano Energy 53 (2018) 596–603, https://doi.org/10.1016/j.nanoen.2018.09.024.

[44] C. Hou, G. Tai, Y. Liu, R. Liu, X. Liang, Z. Wu, Z. Wu, Borophene pressure sensing for electronic skin and human-machine interface, Nano Energy 97 (2022), 107189, https://doi.org/10.1016/j.nanoen.2022.107189.

[45] Y. Yang, J. Han, J. Huang, J. Sun, Z.L. Wang, S. Seo, Q. Sun, Stretchable energy-harvesting tactile interactive interface with liquid-metal-nanoparticle-based electrodes, Adv. Funct. Mater. 30 (2020), 1909652, https://doi.org/10.1002/adfm.201909652.